Concentrations and co-occurrence of 101 emerging and legacy organic pollutants in the ultrafine, fine and coarse fractions of airborne particulates associated with treatment of waste from electrical and electronic equipment

Donatella Pomata [a], Patrizia Di Filippo [a,*], Carmela Riccardi [a], Francesca Buiarelli [b], Federico Marini [b], Leonardo Romani [b], Franco Lucarelli [c], Giulia Pazzi [c], Roberta Galarini [d], Giulia Simonetti [b]

[a] *DIT, Italian Workers' Compensation Authority (INAIL), 00143, Rome, Italy*
[b] *Department of Chemistry, Sapienza University of Rome, 00185, Rome, Italy*
[c] *Department of Physics and Astronomy and INFN, University of Florence, 50019, Sesto Fiorentino, Florence, Italy*
[d] *Experimental Zooprophylactic Institute of Umbria and Marche, 06126, Perugia, Italy*

HIGHLIGHTS

- 101 Flame retardants and plasticizers were detected in the air of e-recycling plants.
- The most detected FR chemical class is organophosphorus compounds (OPEs).
- TPhP predominates among all FRs, with concentrations up to 620 ng/m^3.
- The size distribution of studied chemicals was higher in the ultrafine fraction of PM.
- Organic compound concentrations depend on the amount of waste delivered to the plants.

GRAPHICAL ABSTRACT
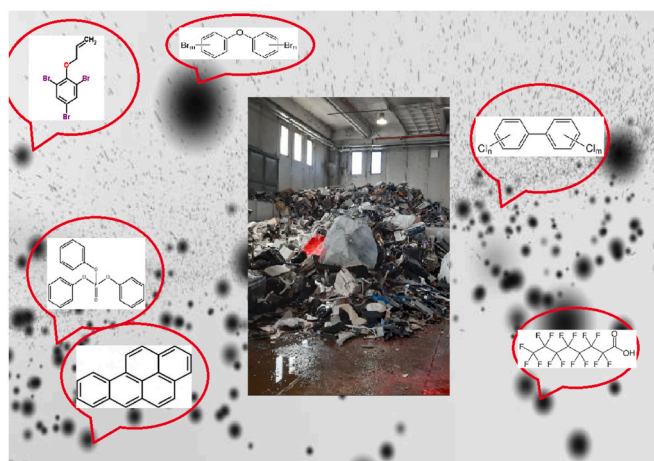
ARTICLE INFO

Handling Editor: R Ebinghaus

ABSTRACT

Occupational exposure to airborne particles can increase the development of morbidity, also because of the chemical composition of particulate matter (PM). In workplace, where manual and mechanical disassembly of electric and electronic equipment (EEE) take place, there are evident risks of respiratory exposure to a great number of different toxic organic compounds present in the electrical and plastic materials of which the

---

* Corresponding author.
  E-mail address: p.difilippo@inail.it (P. Di Filippo).

equipment is made. Airborne particles are numerous, cover a wide range of sizes and are rich in toxic organic compounds. In the present work, a sampling program was conducted and ultrafine, fine and coarse airborne particles were collected in three EEE waste treatment plants. Afterwards, the extraction and analysis of polycyclic aromatic hydrocarbons (PAHs), their nitro and oxygenated derivatives (nitroPAHs, oxyPAHs), organophosphorus compounds (OPEs), Brominated Flame Retardants (BFRs), polychlorinated biphenyls (PCBs), Polybrominated Diphenyl Ethers (PBDEs), and polyfluoralkyl substances (PFASs) was performed. The percentage ratio of the mass of organic compounds and the mass of the ultrafine fraction of PM ($PM_{0.1}$) was higher than those of the fine and coarse fractions. Even with low concentrations, the co-occurrence of numerous potentially toxic compounds capable of easily reaching other organs passing by the lung vasculature, through the lymph makes the working environment unhealthy.

1. Introduction

Electric and electronic equipment contain "legacy" and emergent flame retardants potentially toxic to humans and the environment [Tsydenova and Bengtsson, 2011]. Therefore, in WEEE (Waste Electrical and Electronic Equipment) treatment plants, disassembly and shredding operations can cause the release of airborne particles (PM) containing these toxic chemicals. Both manual and mechanical disassembly and shredding of cell phone shells, computer and TV housings, fluorescent lamps, screens, monitors, washing machines, and other EEE expose workers to contaminants and even in the presence of low concentrations, a cumulative and synergistic effect cannot be excluded [Esplugas et al., 2022].

A previous exploratory study had confirmed the presence of these compounds in airborne fine and coarse particles [Pazzi et al., 2023]. In particular, electronic waste is a source of both legacy (PCBs and PBDEs) and emerging flame retardants (BFRs, OPE, and PFASs).

Moreover, particulate matter of nanoscale size can incidental originate from various working processes and the mechanical processes of abrading, sawing, scratching and shredding leads to a non-negligible percentage of PM is in the range of ultrafine particles (UFPs, aerodynamic diameter less or equal to 100 nm [Buiarelli et al., 2019; López et al., 2022]. Workers' exposure to UFP may be significantly higher than their non-occupational exposure to background concentration alone [Viitanen et al., 2017; López et al., 2022]. Ultrafine PM enters the body through the respiratory system but move to all organs. UFP increased toxicity is due to their high number, their large surface-area and the higher content in organic compounds [Smichowski and Gómez, 2023]. The large variety of compounds making up these particles is likely to be a major cause of their toxicity, and makes difficult to perform a complete speciation.

Besides flame retardants, particles dispersed in a WEEE treatment plant can contain well-known products of incomplete combustion from diesel engine vehicles used for waste handling and delivery [Di Filippo et al., 2010; López et al., 2022].

It is very complex to analyze all those compounds which are numerous and at low concentrations so as to challenge the sensitivity of analytical instruments [Schraufnagel, 2020].

Furthermore, it is also difficult to sample the atmospheric PM with the most commonly used particle collection samplers, since PM concentrations reach more than 1 mg/m³ [Vazquez-Pufleau, 2022]. Therefore, there are few publications related to the occurrence of organic compounds in the airborne particles and particularly in the ultrafine fraction.

The aim of the present work was, then, to collect PM at different size range in three WEEE treatment plants, during different working operations, and proceed with the organic speciation of as many compounds as possible, some of which hazardous, chosen on the basis of the presence of electric and electronic equipment waste and for the diesel emission sources [Roth et al., 2012]. Thus, airborne particulates were extracted in order to identify and quantify polycyclic aromatic hydrocarbons (PAHs), and their nitro and oxygenated derivatives (nitroPAHs, oxyPAHs), and the flame retardants organophosphorus compounds (OPEs), Brominated Flame Retardants (BFRs), polychlorinated biphenyls (PCBs),

Polybrominated Diphenyl Ethers (PBDEs), and polyfluoralkyl substances (PFASs) [Morf et al., 2005; Tsydenova and Bengtsson, 2011; Sonego et al., 2022; Roth et al., 2012; Pazzi et al., 2023].

2. Methods

2.1. Sampling sites

The sampling locations of the airborne particulate matter were chosen according to the activity carried out and the type of waste treated. In particular, in the first plant under study (P1), the waste treatment is carried out in two adjacent warehouses. Zone 1 (P1_Z1) is dedicated to manually disassembly Liquid Crystal Display (LCD) or Cathode Ray Tube (CRT) television (TV), tablets, smartphones; Zone 2 (P1_Z2) is used for crushing glass component of cathode ray tube, flat screen televisions and Personal Computer (PC) monitors by an industrial shredder. In the second plant (P2), waste treatment activities are also carried out in two separate warehouses. Zone 1 (P2_Z1) is a disassembly area, where the workers provide for the manual disassembly of PCs and monitors, and the selection of the recoverable parts (metallic material, non-metallic material, plastics, etc.). Zone 2 (P2_Z2) is a treatment area where small household appliances are break down in an industrial shredder, after a mechanical pre-treatment process to open the appliances and manually separate the recoverable components, before the subsequent shredding phases. In the third plant (P3), the waste processing area is divided into two adjacent areas: Zone 1 (P3_Z1) relating to the washing machine treatment line, where a mechanical milling section performed the size reduction of the appliances and Zone 2 (P3_Z2) where fluorescent tubes and linear lamps are processed through an industrial shredder.

2.2. Sampling Instruments

Particle-phase collection for analysis of PM organic fraction is performed using two low pressure size fractionating Impactors (DLPI+, Dekati, Kangasala, Finland) coupled in series. The DLPI+ classifies and collects particles into 14 size fractions in the range of 16 nm–10 μm, operating at a flow rate of 10 L/min. The particles are collected on 25 mm polycarbonate membrane filters (Sterlitech, 0.8 μm, Rome, Italy) that are weighed before and after the sampling to determine the particle mass. PM_{10} parallel samplings to calculate the standard deviation on the results were performed on Teflon filters (47-mm PTFE filters, polypropylene ring, Millipore Merk, Darmstadt, Germany), with single-stage inertial impactors (SKC IMPACT Sampler, for PM_{10} Sampling; SKC, PA, USA) attached to Legacy sampling pumps operating at 10 L/min (Leland Legacy Sample Pump, SKC, PA, USA).

2.3. Samplings

In P1 and P2, two sampling campaigns are performed (C1 and C2 in P1, C3 and C4 in P2); in P3 one campaign (C5) is carried out. At each of the two zones of the three plants (P1_Z1, P1_Z2, P2_Z1, P2_Z2, P3_Z1, P3_Z2), three sampling episodes per campaign, one episode per day, have been performed. Therefore 3 sampling episodes x 2 zones x 5

campaigns = 30 total episodes are carried out.

Two independent air samplers have been simultaneously utilized during each of the episodes, with 2-h sample runs, at a flow rate of 10 L/min, with an average total collected volume of 1.2 m^3 per sampler. Table 1 provides a summary of the campaigns carried out for three days in each zone of the three sites with the relative abbreviations and the description of the specific WEEE treatment in the sampling site. In P1_Z1, during the first day of C2 campaign, a parallel sampling, carried out with three PM_{10} impactors, lasting 120 min, with a final volume of sampled air equal to 1.2 m^3 and an amount of PM_{10} on each filter of about 0.6 mg, was performed.

2.4. Chemical analysis

In order to determine PM mass concentrations, the filters are weighed before and after sampling, by using a Sartorius MC5 microbalance, following standard protocols.

For organic speciation, after the weighing operation, the filters of the three episodes (six samplers) of the same zone and same campaign are combined to obtain one sample $PM_{0.1}$, one sample $PM_{0.1-1}$ and one sample PM_{1-10}, for a total volume of sampled air equal to 7.2 m^3. Ten $PM_{0.1}$, ten $PM_{0.1-1}$ and ten PM_{1-10} samples, in total, are obtained.

Organic compounds analysis is performed by HPLC/MS-MS (Agilent 1290 and Agilent G6460 with ESI, Agilent Technologies, Santa Clara, CA, US) or GC-MS (Agilent 7890B and Agilent G5977B, Agilent Technologies, Santa Clara, CA, US), after appropriate extraction of organic substances from the particulate matter deposited on filters and purification of the extracts. The analytical method is discussed in detail in previous works [Buiarelli et al., 2017; Simonetti et al., 2020; Pomata et al., 2021; Sonego et al., 2022; Pazzi et al., 2023; Pomata et al., 2020; Buiarelli et al., 2019].

Briefly, samples are extracted by Accelerated Solvent Extraction (ASE, Dionex, ThermoFisher Scientific, Waltham, MA, US) with n-hexane/ethyl acetate, and 2-propanol/methanol. Florisil for clean-up is directly added in the ASE extraction cell. The solutions are concentrated under nitrogen, filtered and reconstituted in methanol for HPLC analysis and toluene for GC analysis. All PFASs and the following OPEs: TEP, TDCPP, TBuP, TIBP, and TBEP are analyzed by HPLC, all the other compounds are analyzed by GC (compound names and corresponding abbreviations can be found in Supplementary Materials). The average organic compound concentrations in field blanks, higher than method LOQs, are subtracted from sample results. As not all internal standards are available, and because liquid chromatography-tandem mass spectrometry is subject to matrix effects, matrix-matched calibration curves are constructed for each sampling site. Since samples containing the matrix alone were not available, the multistage impact filters (six) corresponding to the last stage were spiked with multi-standard at growing concentrations and treated according to the method. The calibration curves were obtained by subtracting the environmental value, obtained by extrapolation of the regression line, to each point of the curve.

2.5. Statistical studies

The standard deviation (SD) calculated on the organic compound concentration results was not applicable since all the samplings performed in parallel together with those performed on three successive days at the same sampling site have been extracted as a single sample (see § Sampling). Therefore, the SD associated with the measurements is the dispersion of the values obtained on three PM_{10} samples collected in parallel with three single-stage inertial impactors (see 'Sampling Instruments' and 'Samplings' Sections). The sampled filters were extracted and analyzed as described in Section 'Chemical analysis'.

T-test was applied to the results in order to compare the results.

Pearson's correlation coefficient was calculated to assess the degrees of relations among the classes of compounds identified in the sites under study.

Source apportionment was carried out by multivariate curve resolution-alternating least squares (MCR-ALS) [De Juan et al., 2014] applied by the multiset data obtained by concatenating row-wise the three matrices corresponding to the composition of $PM_{0.1}$, PM_1 and PM_{10}. Number of components for the optimal MCR decomposition was chosen based on preliminary PCA analysis and on chemical interpretability of the solution. Resolution was accomplished by imposing non-negativity constraint on both the relative contribution and the chemical profiles and closure (mass-balance) to the relative contributions.

3. Results and discussion

3.1. Ultrafine, fine and coarse fractions of the airborne PM

Fig. 1 summarizes the mass concentrations in $\mu g/m^3$ of the ultrafine, fine and coarse fractions of the airborne PM obtained on average in the 5 campaigns carried out in the 3 different sites each of which with 2 different processes (see the summary of the campaigns in Table 1). The lower bars of the histograms indicate the $PM_{0.1}$ concentrations, while the dotted upper parts indicate the PM_{1-10} concentrations.

Ultrafine fraction mass concentrations ranged from 12 $\mu g/m^3$ in

Table 1
Summary of the sampling campaigns: abbreviations of the sampling locations and description of the working operations.

| Plants	Campaigns	Episodes	Sample abbreviations	Description of WEEE treatment
P1	C1	9-10-11 DEC 2020	P1_Z1_C1	disassembly of PCs and monitors
	C2	12-13-14 OCT 2021	P1_Z1_C2	
	C1	9-10-11 DEC 2020	P1_Z2_C1	shredding of glass components
	C2	12-13-14 OCT 2021	P1_Z2_C2	
P2	C3	24-25-26 MAY 2021	P2_Z1_C3	disassembly of PCs and monitors
	C4	22-25-24 FEB 2022	P2_Z1_C4	
	C3	24-25-26 MAY 2021	P2_Z2_C3	shredding of small household appliances
	C4	22-25-24 FEB 2022	P2_Z2_C4	
P3	C5	28-30 JUN 2022	P3_Z1_C5	mechanical milling of washing machine
	C5	28-30 JUN 2022	P3_Z2_C5	shredding of fluorescent tubes and linear lamps
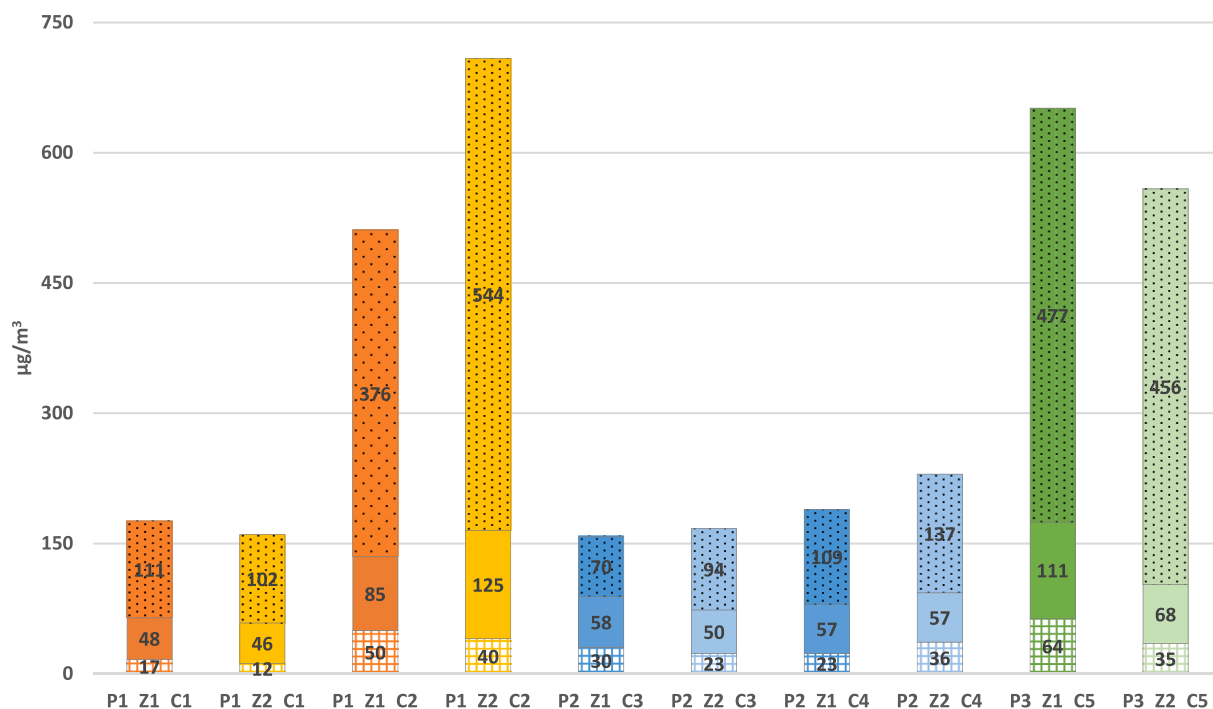
Fig. 1. Concentrations in µg/m³ of the ultrafine, fine and coarse fractions of airborne particles in each sampling site (values shown in figure). The dotted part of the bars is relative to the coarse fraction, the checkered one shows the ultrafine concentration.

P1_Z2_C1 to 64 µg/m³ in P3_Z1_C5. Ultrafine mass concentrations in WEEE treatment facilities is only reported in a previous study [Buiarelli et al., 2019]; the literature does not provide any other information about UFP mass concentration in these workplaces. In a review about workers' exposure to ultrafine particles in various work environments, concentrations are given in particle number (n/cm³), having been used particle counters [Viitanen et al., 2017 and references therein]. If the work environments where engineered nanoparticles are present are excluded, ultrafine particle occupational mass concentrations are investigated in a few workplaces. UFP mass concentrations were investigated in metal polishing/buffing, spot welding, and milling operations, as sources of solid metal particles, fume aggregates and metalworking fluid mists, where a maximum of 24.4 µg/m³ was found [Young et al., 2013]. A concentration of 19.5 µg/m³ was found in a Wire Electrical Discharge Machining Workshop [Chen et al., 2015]. Ambient ultrafine particles at urban sites are much more studied and mostly show concentrations lower than 3.5 µg/m³ [Cabada et al., 2004; Sardar et al., 2005; Di Filippo et al., 2010].

In the present study, the ultrafine fraction percentage with respect to PM_{10} is comparable in P1 and P3 (range 5.6–9.8%) and higher in P2 (range 12.2–19.0%), depending on the higher (P1 and P3) or lower (P2) concentration of the coarse fraction. On average, the mass percentage of ultrafine fraction in PM_{10} of 11% is higher than in urban atmospheres where is generally less than 5% and where the main source is the incomplete combustion of carbon containing materials [Cabada et al., 2004; Di Filippo et al., 2010; Gugamsetty et al., 2012]. This higher percentage is mainly due to the concentration of the coarse fraction. In all samples, PM_{1-10} mass concentrations contribute more to PM_{10}. PM_1 concentrations, obtained as the sum of the ultrafine and fine particles, range from 58 to 175 µg/m³, while the concentrations of PM_{10} obtained as the sum of the fine and coarse particles show the range 158–709 µg/m³. PM_{10} concentrations lower than 400 µg/m3 were found near the dismantling area in a WEEE treatment plant, located in central Greece, where the fluctuations of PM_{10} were associated with both PM_{10} emissions and resuspension of dust [Papaoikonomou et al., 2018]. Kim in 2015 measured indoor PM_{10} concentrations in a modern U.S.-based e-waste recycling facility. The result range from 220 to 1200 µg/m³

reflected no clear relationship between waste streams, activity level (on or off) of processing lines and particle mass concentrations. Instead, the authors attributed the PM concentration fluctuations to material movement activities within the workspace (constant motion of e-waste with fork lifts and front-end loaders) [Kim et al., 2015]. In the present study, the four higher PM_{10} values (P1_Z1_C2, P1_Z2_C2, P3_Z1_C5, P3_Z2_C5), depending on the coarse fraction, as can be seen from Fig. 1, are most likely due to dust resuspension. The different working operations do not cause higher or lower concentrations of either fine or coarse PM. The difference between the campaigns C1 and C2 in P1_Z2 is due to two main factors; during C2 campaign, the amount of waste delivered to the plant was particularly high and the shredding of glass components of monitors was at full power (capacity). On the contrary, during C1 campaign the shredder was undergoing routine maintenance.

3.2. Classes of organic compounds in ultrafine, fine and coarse fractions

One hundred and one organic compounds from the classes PAHs, nitroPAHs, oxyPAHs, OPEs, BFRs, PCBs, PBDEs, and PFASs have been identified in airborne particulate fractions $PM_{0.1}$, $PM_{0.1-1}$ and PM_{1-10}. Names and concentrations are listed in Supplementary Material in Tables S1 and S2.

Fig. 2a shows the concentrations of total organic compounds obtained from the sum of all determined analytes in size-segregated airborne particles, sampled in the two zones of the three sites during the five monitoring campaigns. Ultrafine organic particle concentrations are in the range 96–342 ng/m³, $PM_{0.1-1}$ organic particle concentrations are in the range 69–486 ng/m³, while in the PM_{1-10} fraction the range of organic compound concentrations is 130–451 ng/m³. The contribution of organic contaminants to airborne fine particle mass concentrations ($PM_{0.1}+PM_{0.1-1}$) is higher, on respect organic in PM_{1-10} (see Table S3 in Supplementary material with concentrations ± SD).These findings are in total contrast with Nguyen et al. (2019). The authors found >70% of total airborne FR mass in particles ranging from 3.2 to 18 µm diameter and conversely, 30% were in respirable particles (<~3 µm diameter). The most abundant size fraction in terms of total airborne FR concentrations was on inhalable particles 3.2–5.6 µm diameter.
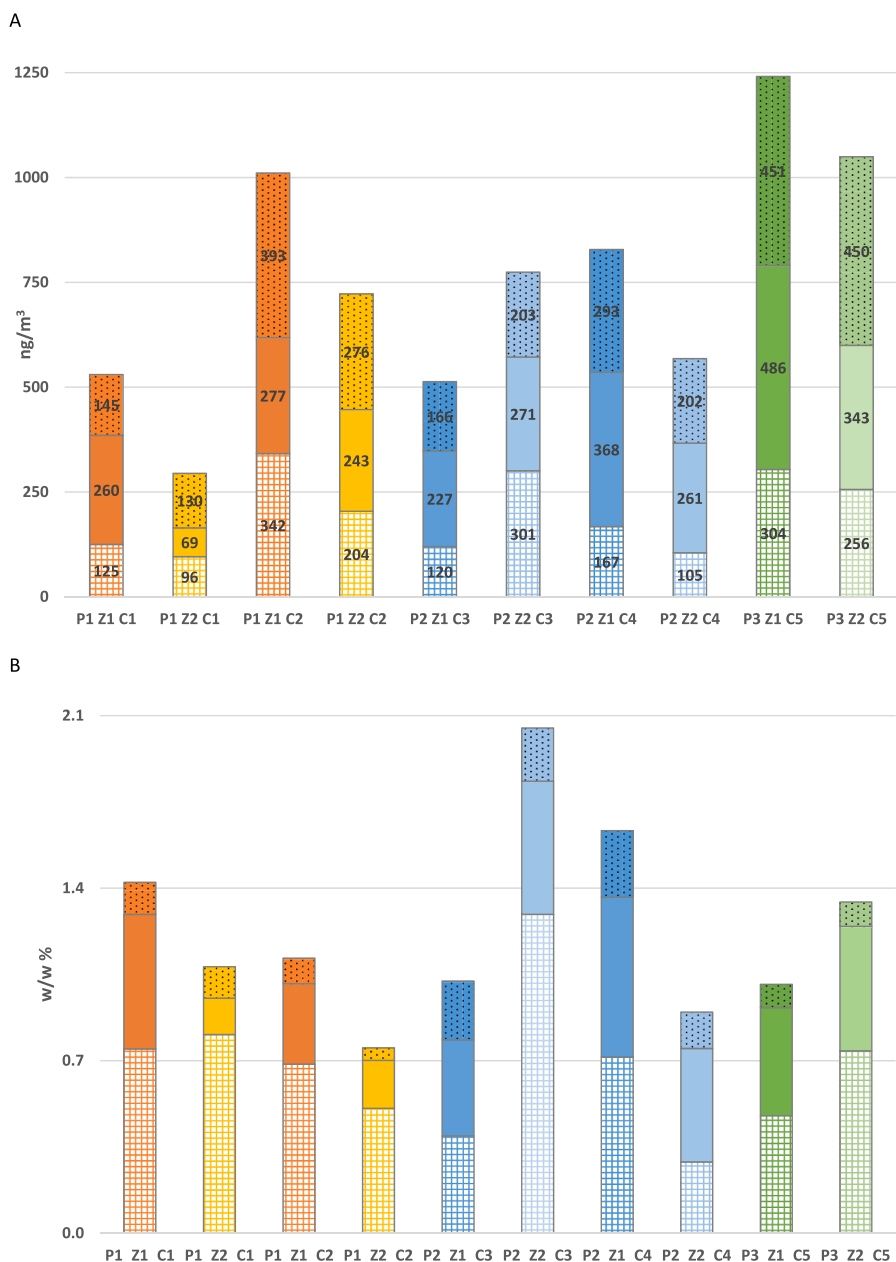
A

B

Fig. 2a. Fig. 2a. Concentrations in ng/m^3 of the sum of all organic compounds found in the ultrafine, fine and coarse fractions of airborne particles.

The dotted upper part of the histogram is relative to the coarse fraction, the checkered one shows the ultrafine concentration, the central part illustrates the concentrations of organic compounds in the 0.1–1 fraction.

Fig. 2b. Percent by weight calculation of organic substances in ultrafine, fine and coarse PM.

Excluding the low organic concentration in P1_Z2_C1 due to the stoppage of shredding operations, for maintenance, lower concentrations (statistically significant as confirmed by *t*-test in Table S4 in Supplementary Material) are in P1_Z1_C1 and P2_Z1_C3, where manual operations are performed. By comparing P1_Z1_C1 and P1_Z1_C2, where the same operation takes place, concentrations are higher in the second campaign. The two campaigns, carried out at two different periods, in the same place, demonstrate that neither the airborne PM amount nor the organic substance content depend on the processing. Conversely, the types and quantity of material delivered affect the airborne pollutants, as already highlighted by Balasch et al. (2022).

Also depending on the types of material treated, which is daily variable, the highest content of organic substances with low concentrations of PM is found in the P2 plant, as shown in Fig. 2b, reporting percent organic in particulate matter, calculated as the ratio of weight of extracted organic compounds and weight of particulate x 100. Organic contribution to PM_{10} is in the range of 0.75–2.05% with a major contribution to ultrafine PM (up to 1.3%), except for P2_Z2_C4, the only

sample showing a higher percentage distribution in $PM_{0.1-1}$ on respect $PM_{0.1}$ fraction (see Table S5 in Supplementary material with percentage ± SD). Ultrafine fraction contains a higher percentage of extracted organic compounds, as expected because it is known that large surface area and high surface reactivity enable UFPs to adsorb, for a given mass of PM, greater quantities of hazardous compounds [Kwon et al., 2020].

Table 2 reports the concentrations in ng/m^3 of each class of compounds, obtained from the sum of the concentration of any single compound identified, in the three fractions of PM of each sample with the standard deviation (SD). In all samples except for $PM_{0.1-1}$ of P1_Z2_C1, OPEs are present at the highest concentrations. In the fraction PM_1 as sum of $PM_{0.1}$ and $PM_{0.1-1}$ we found a minimum of 66 and a maximum of 508 ng/m^3 of OPEs as sum of 10 compounds, in PM_{1-10} we found a minimum of 101 and a maximum of 346 ng/m^3 of OPEs as sum of 10 compounds. A concentration equal to 215 ng/m^3 of OPEs as sum of 5 compounds was found in Canada (airborne particle diameter range 0.05–18 μm) inside a WEEE facility, in a central workplace where no dismantling activities were performed [Nguyen et al., 2019]. The

Table 2
Concentrations in ng/m^3 of classes of organic compounds in each fraction of PM in the two zones inside the three sampling sites in all campaigns.

	$PM_{0.1}$ P1 Z1 C1	$PM_{0.1}$ P1 Z1 C2	$PM_{0.1}$ P2 Z1 C3	$PM_{0.1}$ P2 Z1 C4	$PM_{0.1}$ P1 Z2 C1	$PM_{0.1}$ P1 Z2 C2	$PM_{0.1}$ P2 Z2 C3	$PM_{0.1}$ P2 Z2 C4	$PM_{0.1}$ P3 Z1 C5	$PM_{0.1}$ P3 Z2 C5
PAHs	15.117 ± 0.895	54.131 ± 3.163	14.123 ± 0.791	5.494 ± 0.334	12.032 ± 0.716	45.365 ± 2.715	28.607 ± 1.713	4.371 ± 0.263	74.662 ± 4.720	46.502 ± 2.476
OPE	63.566 ± 9.098	118.057 ± 13.063	91.821 ± 14.833	87.649 ± 13.081	54.372 ± 8.299	112.515 ± 12.256	249.703 ± 28.329	88.898 ± 12.460	200.837 ± 26.470	177.280 ± 26.210
N-PAHs	0.093 ± 0.006	0.542 ± 0.072	0.129 ± 0.003	0.043 ± 0.006		0.542 ± 0.098	0.122 ± 0.003	0.190 ± 0.031	1.538 ± 0.332	0.684 ± 0.079
Oxy-PAHs	12.411 ± 1.208	10.262 ± 0.351	5.409 ± 0.184	1.551 ± 0.135	8.739 ± 0.787	7.663 ± 0.139	9.821 ± 0.345	0.907 ± 0.068	19.105 ± 1.146	18.662 ± 1.419
BFRs	22.895 ± 4.373	3.416 ± 0.324	2.872 ± 0.266	1.936 ± 0.161	17.241 ± 3.306	2.748 ± 0.291	4.036 ± 0.341	1.777 ± 0.149	4.278 ± 0.383	5.376 ± 0.430
PBDEs	0.126 ± 0.004	0.306 ± 0.013	3.364 ± 0.165	4.247 ± 0.329	0.056 ± 0.003	0.401 ± 0.022	4.536 ± 0.249	5.282 ± 0.398	0.589 ± 0.020	1.414 ± 0.056
PCBs	0.357 ± 0.031	3.355 ± 0.363	1.714 ± 0.209	1.224 ± 0.143	0.172 ± 0.010	2.478 ± 0.195	2.112 ± 0.222	0.953 ± 0.086	1.686 ± 0.172	2.223 ± 0.187
PFASs	10.457 ± 1.936	151.513 ± 23.882	0.613 ± 0.088	65.325 ± 11.318	3.259 ± 0.562	32.284 ± 4.023	1.646 ± 0.236	2.910 ± 0.415	1.155 ± 0.165	4.105 ± 0.588

	$PM_{0.1-1}$ P1 Z1 C1	$PM_{0.1-1}$ P1 Z1 C2	$PM_{0.1-1}$ P2 Z1 C3	$PM_{0.1-1}$ P2 Z1 C4	$PM_{0.1-1}$ P1 Z2 C1	$PM_{0.1-1}$ P1 Z2 C2	$PM_{0.1-1}$ P2 Z2 C3	$PM_{0.1-1}$ P2 Z2 C4	$PM_{0.1-1}$ P3 Z1 C5	$PM_{0.1-1}$ P3 Z2 C5
PAHs	23.632 ± 1.215	56.779 ± 3.125	19.538 ± 1.155	7.655 ± 0.511	19.341 ± 0.967	66.741 ± 4.626	26.391 ± 1.513	5.264 ±	122.561 ± 7.127	31.781 ± 1.710
OPE	163.295 ± 27.777	104.367 ± 11.391	186.448 ± 31.408	120.400 ± 17.372	11.656 ± 1.433	125.257 ± 15.919	208.489 ± 28.891	219.040 ± 19.210	307.244 ± 42.023	259.049 ± 37.649
N-PAHs	1.298 ± 0.229	0.885 ± 0.146	0.140 ± 0.003	0.201 ± 0.033	0.018 ± 0.002	0.871 ± 0.163	0.205 ± 0.009	0.509 ± 0.082	1.853 ± 0.205	1.131 ± 0.117
Oxy-PAHs	31.981 ± 3.913	12.253 ± 0.379	6.212 ± 0.230	1.319 ± 0.068	18.431 ± 2.045	13.355 ± 1.634	10.319 ± 0.510	1.177 ± 0.082	39.534 ± 2.214	32.762 ± 3.607
BFRs	33.800 ± 6.482	4.806 ± 0.485	3.505 ± 0.306	3.695 ± 0.300	16.787 ± 3.230	3.451 ± 0.344	5.642 ± 0.476	4.223 ± 0.295	5.559 ± 0.391	7.028 ± 0.566
PBDEs	0.166 ± 0.007	0.468 ± 0.019	7.193 ± 0.283	14.275 ± 0.882	0.017 ± 0.001	0.440 ± 0.023	12.415 ± 0.415	14.430 ± 0.858	3.527 ± 0.202	1.642 ± 0.083
PCBs	0.707 ± 0.060	1.780 ± 0.204	3.590 ± 0.441	1.107 ± 0.100	0.232 ± 0.015	1.719 ± 0.150	6.263 ± 0.693	1.938 ± 0.137	3.187 ± 0.252	5.746 ± 0.574
PFASs	5.225 ± 0.997	95.320 ± 14.108	0.718 ± 0.103	219.523 ± 38.150	2.072 ± 0.368	30.672 ± 4.114	1.472 ± 0.211	14.708 ± 2.396	2.638 ± 0.378	4.275 ± 0.612

	PM_{1-10} P1 Z1 C1	PM_{1-10} P1 Z1 C2	PM_{1-10} P2 Z1 C3	PM_{1-10} P2 Z1 C4	PM_{1-10} P1 Z2 C1	PM_{1-10} P1 Z2 C2	PM_{1-10} P2 Z2 C3	PM_{1-10} P2 Z2 C4	PM_{1-10} P3 Z1 C5	PM_{1-10} P3 Z2 C5
PAHs	12.942 ± 0.806	49.675 ± 3.040	15.947 ± 0.896	7.173 ± 0.454	8.977 ± 0.582	88.162 ± 5.362	23.957 ± 1.435	5.340 ± 0.351	63.988 ± 3.973	49.750 ± 2.655
OPE	100.616 ± 11.243	198.470 ± 17.004	123.624 ± 17.699	135.913 ± 20.365	106.390 ± 15.015	123.709 ± 16.295	147.218 ± 21.071	134.322 ± 18.798	346.303 ± 43.990	332.726 ± 46.701
N-PAHs	0.108 ± 0.016	0.427 ± 0.097	0.143 ± 0.003	0.101 ± 0.018		0.444 ± 0.069	0.158 ± 0.003	0.236 ± 0.048	0.074 ± 0.007	2.341 ± 0.149
Oxy-PAHs	6.115 ± 0.438	9.757 ± 0.415	5.670 ± 0.138	1.541 ± 0.112	2.976 ± 0.122	24.758 ± 1.891	9.073 ± 0.415	1.358 ± 0.110	22.927 ± 1.327	27.856 ± 2.796
BFRs	13.581 ± 2.325	5.509 ± 0.455	4.302 ± 0.280	5.848 ± 0.556	6.259 ± 1.255	14.424 ± 2.157	5.196 ± 0.418	5.176 ± 0.331	8.566 ± 0.628	14.087 ± 1.178
PBDEs	0.157 ± 0.005	1.287 ± 0.055	13.429 ± 0.509	14.462 ± 0.973	0.091 ± 0.005	0.930 ± 0.040	12.589 ± 0.463	40.500 ± 2.976	2.401 ± 0.080	8.401 ± 0.335
PCBs	0.191 ± 0.011	1.857 ± 0.196	1.926 ± 0.232	1.410 ± 0.147	0.042 ± 0.002	1.595 ± 0.169	2.772 ± 0.251	3.630 ± 0.239	3.582 ± 0.302	9.401 ± 0.472
PFASs	11.318 ± 1.994	125.615 ± 20.308	0.840 ± 0.120	126.250 ± 21.914	5.314 ± 0.928	21.827 ± 2.271	1.638 ± 0.234	11.001 ± 1.663	3.154 ± 0.451	5.020 ± 0.719

presence of airborne microplastic from the disassembly of small household appliances could be the cause of a greater quantity of OPEs in the airborne dust. It has been estimated that plastic concentrations are about 9% in large household appliances, 48% in small household appliances, 30% in ICT equipment, and 31% in TV, radio and similar appliances, of the total weight of these devices [Fjäder et al., 2022]. Additionally, the high OPE concentration in P3 Z2, where linear lamps and fluorescent tubes are shredded, can be due to OPE occurrence in poly(methylmethacrylate) that is a material used for lamps.

For the other classes of compounds, they are more or less concentrated depending on the site, the campaign and the fraction of PM. PBDEs are noteworthy for their higher concentration only in P2 (statistically significant as confirmed by t-test in Table S4 in Supplementary Material), where the concentrations found were more than an order of magnitude lower than data reported by Kim et al. (2015), but higher on respect concentrations reported by Morin et al. (2017). The PBDEs have been used in resins and polymers, in particular PVC and polypropylene; both materials, widely used in Europe, were mostly added with PBDEs as flame retardants [Rahman et al., 2001]. The reason why the PBDE concentrations are so higher in P2 can only be attributed to the type of waste treated in the plant. Some polymers used in EEE, as acrylonitrile butadiene styrene (ABS), and high impact polystyrene (HIPS) are treated with PBDEs in order to meet fire safety regulations [Stubbings et al., 2021; Chaine et al., 2022]. The increasing use of other additives as substitutes to phased-out PBDEs and PCBs as flame retardants and/or plasticizers, is not yet observable in this plant where old equipment is apparently delivered. The presence of PBDEs in WEEE plastics is a well known problem, as it limits the possibility of recycling [Strobl et al., 2021].

Polychlorinated biphenyls are an important class of commercial chemicals widely used in various industrial applications and, although banned since 1979 and included in the Stockholm Convention's list of persistent organic pollutants, they continue to be present due to the recycling stream of electronic waste [Shi et al., 2019]. In the sites under study, PCB concentration associated with PM_{10} particulate matter in the range of 0.5–17 ng/m^3 is lower if compared with concentrations found in WEEE collecting facilities in Norway (9–195 ng/m^3) in 2017 [Arp et al., 2020], reflecting the effectiveness of European restrictive regulations. PCBs give a more significant contribution in the first campaign in P2 (P2_Z1), as well as in P3_Z2. The transfer of old equipment and/or EEE from countries with less restrictive policies towards flame retardants may be the cause of their high content in the airborne dust sampled in P2. Moreover, light ballasts for fluorescent lamps are potentially important sources of PCBs [Montano et al., 2022], which explains their non-negligible concentration in P3_Z2.

A greater contribution can instead be observed for the BFRs (PM_{10} concentration range 11–70 ng/m^3). The increasing use of BFRs as substitutes to phased-out PBDEs and PCBs as flame retardants and/or plasticizers [Sharkey et al., 2020], is observable in P1, where BFRs are higher during the first campaign C1 with a peak of 23 ng/m^3 in the ultrafine fraction. Brominated flame retardants are present in small brown goods, in IT equipment, and cell phones.

NitroPAH and oxyPAH concentrations are at least one order of magnitude higher than those reported in urban outdoor atmosphere [Di Filippo et al., 2010; Di Filippo et al., 2015]. Since in these warehouses, waste is handled using diesel-powered vehicles, part of these compounds can derive from direct emissions. OxyPAH concentrations are higher in P3, mainly caused by 1,8-naphthalic anhydride, as will be seen below. Since 1,8-naphthalic anhydride is known to be an oxidation product of the reactions of three-ring PAHs, it can be hypothesized an emission due to many oxidizing species on the particle surface in P3 [Weschler, 2011; Jiang et al., 2019].

PFASs show the widest concentration range, with a minimum equal to 2 and a maximum equal to 411 ng/m^3 in PM_{10} (obtained by the sum of the three fractions). Higher concentrations of PFASs are detected in the second campaign of P1_Z1 and in the second campaign of P2_Z1 (372 and 411 ng/m^3 respectively), where manual disassembly takes place.

Mostly, PFASs have been incorporated into such a wide range of products that it makes it difficult to understand their provenance when they are identified in environment. A main use of perfluorocarboxylic acids is in the production of fluoropolymers, which are high-performance plastics resistant to acids, alkalis and solvents, suitable as insulating materials of wiring in connector assemblies and cables and gears, slide plates, gaskets and a series of common applications

[Lindstrom et al., 2011]. Due to the PFAS negligible volatilization [Sima and Jaffé, 2021], their presence in air can be mostly caused through emissions of contaminated particles.

Pearson correlation coefficients (See Table S6 in the Supplementary Material) applied to the classes of organic compounds identified in PM_{10} (obtained as the sum of the concentrations found in $PM_{0.1}$, $PM_{0.1-1}$, PM_{1-10}) showed a significant correlation of PAHs with OPEs, N-PAHs, and Oxy-PAHs; of OPEs with N-PAHs, Oxy-PAHs, and PCBs. A poor correlation was found for BFRs, PBDEs, and, above all, PFASs with all the other classes of compounds. PAHs, N-PAHs, and Oxy-PAHs had been chosen as indicators of incomplete combustion, while OPEs should be present for their use as flame retardants. This result instead implies that both a common source and additional sources contribute to PAH, N-PAH, and Oxy-PAH occurrence.

3.3. Relative proportion of individual congeners in relation to the total for each class of compounds in PM_{10}

Within the same class of compounds, the identified analytes show very different concentrations, and a few of them weigh more than the others. Therefore, the histograms of Figs. 3–10 illustrate the amount of each compound relative to the others of the same class. The figures refer to the compounds found in PM_{10} because there are no significant differences, regarding organic distribution, among the three fractions.

The histogram in Fig. 3 shows that the most abundant OPE is always triphenylphosphate (TPhP; concentration range in PM_{10} 137–620 ng/m^3); this result is in line with what has already been reported in the literature [Stubbings et al., 2019]. TPhP is a known additive with the functions of flame retardant and/or plasticizer in the plastic material of computers, computerized video display units (VDU), in coolants in refrigerators and oil-filled electric heaters and hydraulic fluids [Suresh et al., 2018; Balasch et al., 2022]. TPhP is suspected to be an endocrine disruptor. Therefore, the concentration in the range of 46–147 ng/m^3 found on ten samples in the ultrafine fraction of particles does not necessarily guarantee occupational health and safety, especially if exposure continues throughout the working life and if other toxic substances coexist.

The histogram in Fig. 4 shows the PAH percentages. Of particular interest is the PAH-profile, different from that of previous studies, which report a predominance of HMW PAHs [Di Filippo et al., 2010]. Phenanthrene is the most concentrated PAH (range in PM_{10} 11–155 ng/m^3),

with an average percentage of 69%. Fluoranthene (concentration range 2–26 ng/m^3) and pyrene (concentration range 1–19 ng/m^3) have an average percentage of 13 and 2%, respectively.

Crude oil and extender oils are sources of PAHs in the process of manufacturing plastic matrices. PAHs can be found as impurities in crude oil, extender oils, and carbon black. The latter is used as reinforcing filler in rubber formulations or as pigment in plastics; extender oils are used as plasticizer oils and softeners [Lassen et al., 2012].

In addition, products made from post-commercial waste recycled polyethylene contain high concentrations of PAHs and of phenanthrene in particular, present as an impurity.

Anthracene paste or oil can be used as sealants and corrosion protectors. This formula provides for the presence of both phenanthrene and anthracene. Anthracene can be used for light emitting diodes (LEDs), showing a behavior as semiconductor. Anthracene is also used as an additive for paints and can be found in colored parts of white appliances and electronic equipment [Cattley et al., 2023].

Moreover, fluoranthene and pyrene have been detected at very high concentrations in polypropylene samples on which mechanical recycling has been applied. Mechanical recycling is the most widely employed recycling process to treat primary (industrial) and secondary (post customer) plastic waste in Europe, for the recovery of materials including polyethylene, polypropylene and polyethylene terephthalate [Alassali et al., 2020]. Finally, low-ring PAHs are detected at important amounts in polystyrene samples, with phenanthrene as the PAH at the highest average concentration [Li et al., 2017].

Therefore, low molecular weight PAH concentrations and PAH profile indicate a source of PAHs other than incomplete combustion, and plastic consumer products can be a source.

Phenanthrene, anthracene and pyrene are not classifiable as to their carcinogenicity to humans, yet a metabolic activation of phenanthrene and pyrene, but not its isomer anthracene, in humans is demonstrated, with evident metabolite-dependent hepatotoxicity both in mice than and in the rat, but not yet in humans [Schober et al., 2010; Yang et al., 2019]. About thirty percent of these three compounds (range 4–48 ng/m^3, as a sum of the three) are distributed in the ultrafine fraction, therefore a greater attention should be paid to their occurrence in air.

The histogram in Fig. 5 shows the PBDE relative proportion in PM_{10}. The most abundant PBDEs are BDE153 (max value found 55 ng/m^3), BDE28 (max value found 33 ng/m^3), BDE99 (max value found 22 ng/m^3), BDE100 (max value found 35 ng/m^3), and BDE47 (max value found
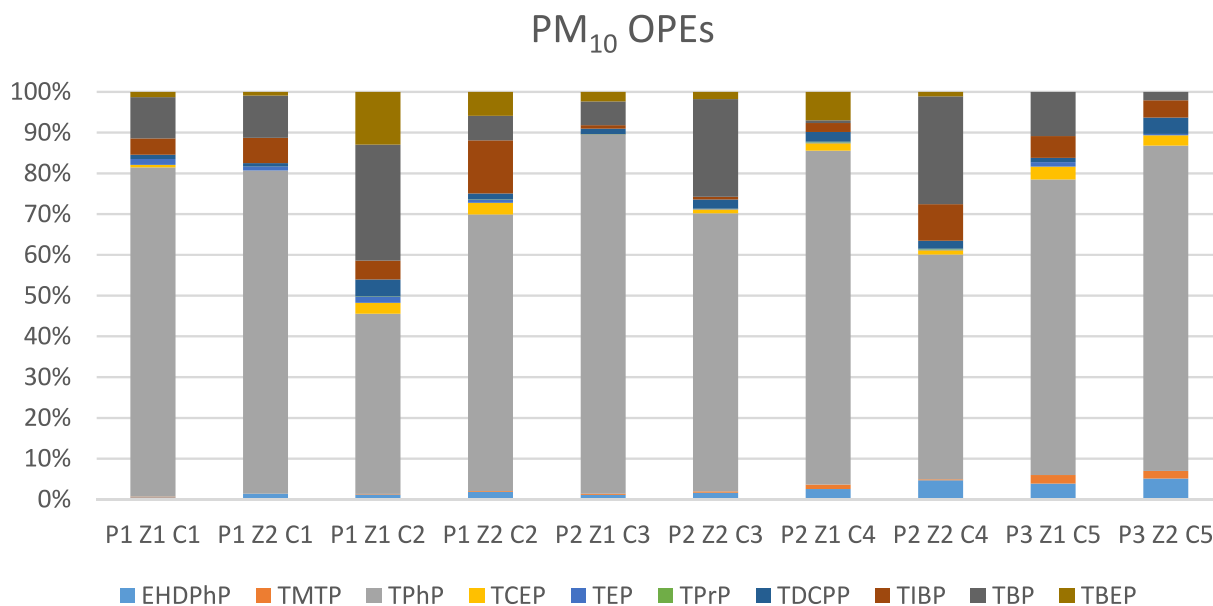

Fig. 3. 11. Percentage of each compound to the total OPEs in PM_{10} (compound names and corresponding abbreviations can be found in Supplementary Materials).
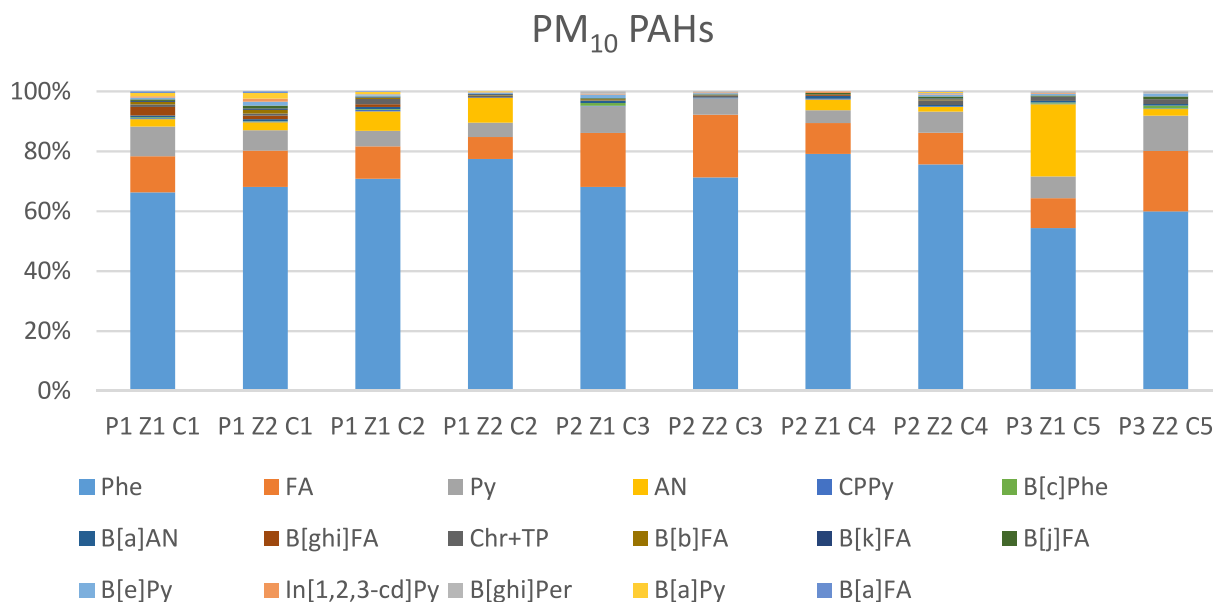
PM$_{10}$ PAHs

Fig. 4. Percentage of each compound to the total PAHs in PM$_{10}$ (compound names and corresponding abbreviations can be found in Supplementary Materials).
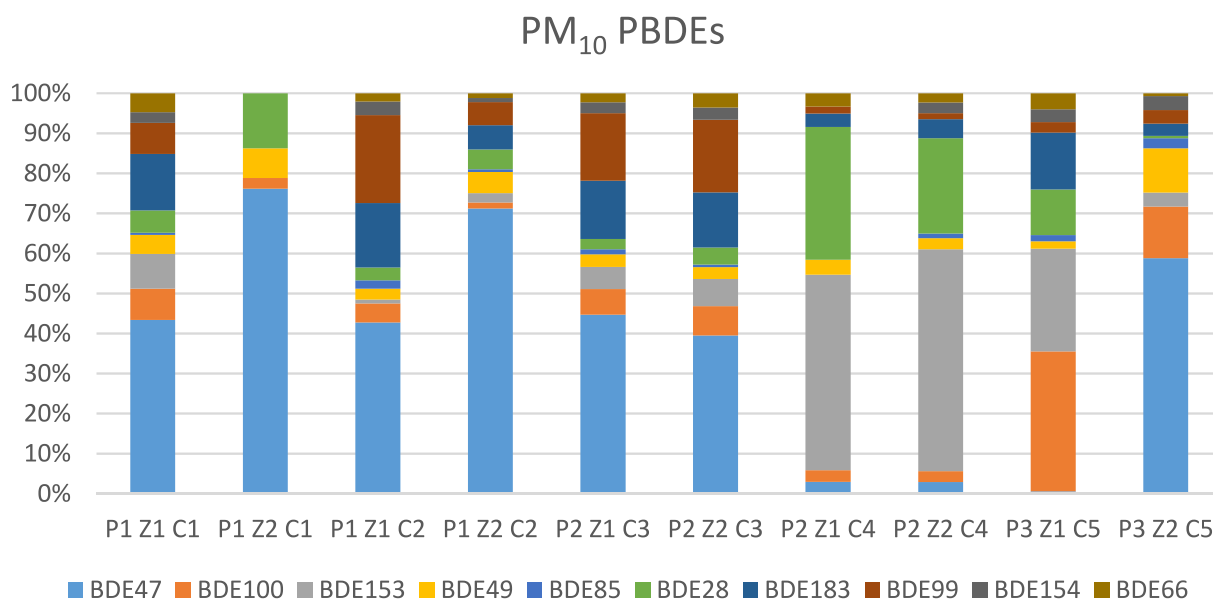
PM$_{10}$ PBDEs

Fig. 5. Percentage of each compound to the total PBDEs in PM$_{10}$.

76 ng/m^3), with BDE47 at the highest percentage in seven of the 10 samples. Computer, radio, and television cabinets can contain PBDEs used as flame retardants in plastics, furniture, and other household products. As known, humans can metabolize some PBDEs into the hydroxylated forms, which is a concern due to greater health risks associated with OH-PBDEs. In the present study, we do not report the concentrations of BDE 209, which notoriously dominates among other PBDEs in air samples of WEEE facilities [Stubbings et al., 2019], representing 85% of a total of 34 PBDE congeners. Therefore, the concentration of this class of compounds, ranging between 0.053 and 5.282 ng/m^3, is probably affected by this deficiency and is not comparable with other results in the literature.

The histogram in Fig. 6 shows the PCB congeners relative proportion. PCB 110 predominates over other PCBs and based on data from in vitro studies, it is among the most neurotoxic congeners [Candelmo et al., 2010]. The concentration range found is 3.3–9.0 ng/m^3 with the maximum at P3_Z2. In fact, the ballasts (or reactors) used in the field of

lighting (electronic circuits designed to drive discharge lamps, generally fluorescent) contained in the condenser Aroclor 1242 and 1248, mixtures of biphenyl polychlorinates. An association between exposure to PCBs and increased incidences of cancer has been demonstrated [Safe, 1997]. OSHA permissible exposure limits (PEL) is 1 mg/m^3 for chlorodiphenyl products containing 42% chlorine and 0.5 mg/m^3 for chlorodiphenyl products containing 54% chlorine determined as 8-h time-weighted average (TWA) concentrations. No more of 17 ng/m^3 were found in PM$_{10}$ of the atmospheres under study, of which 1.7 ng/m^3 in ultrafine particles.

The histogram in Fig. 7 shows the BFR congeners relative proportion found in PM$_{10}$. Among the most abundant BFRs, TBCO (PM$_{10}$ concentration range 0.9–12.3 ng/m^3) and ATE (PM$_{10}$ concentration range 1.3–2.5 ng/m^3) are highly efficient flame retardants, used in expanded polystyrene (mainly used in rubber, compounds for electrical insulation, in computer, video and telephone enclosures, and in components for air conditioners) often used in place of the HBCD, and the PBDEs,
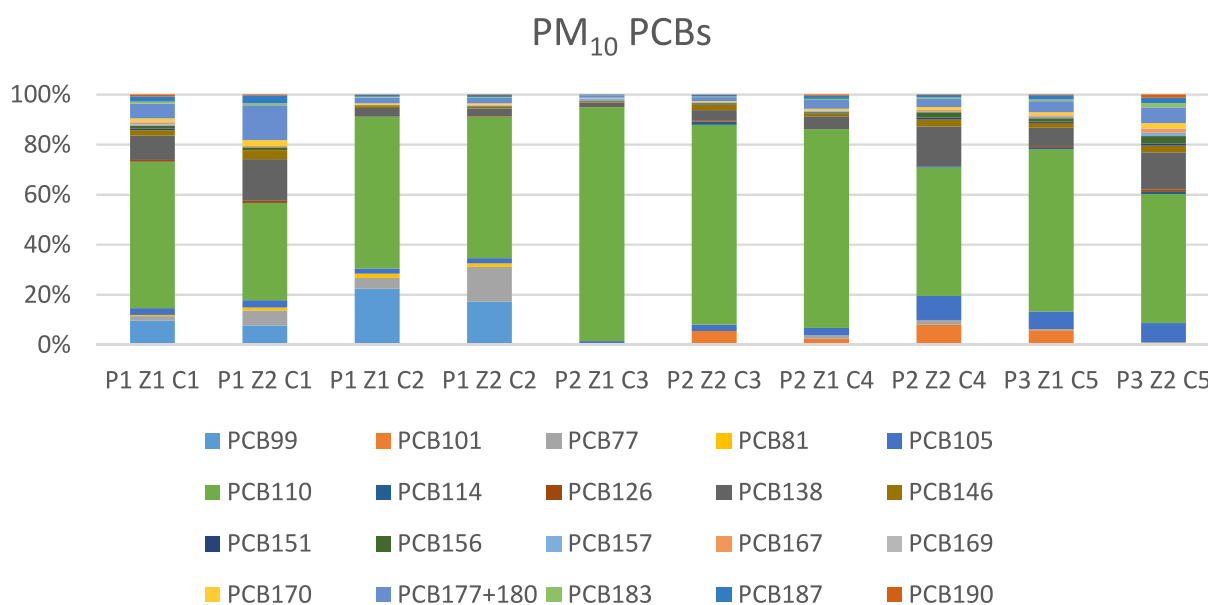
PM$_{10}$ PCBs

Fig. 6. Percentage of each compound to the total PCBs in PM$_{10}$.
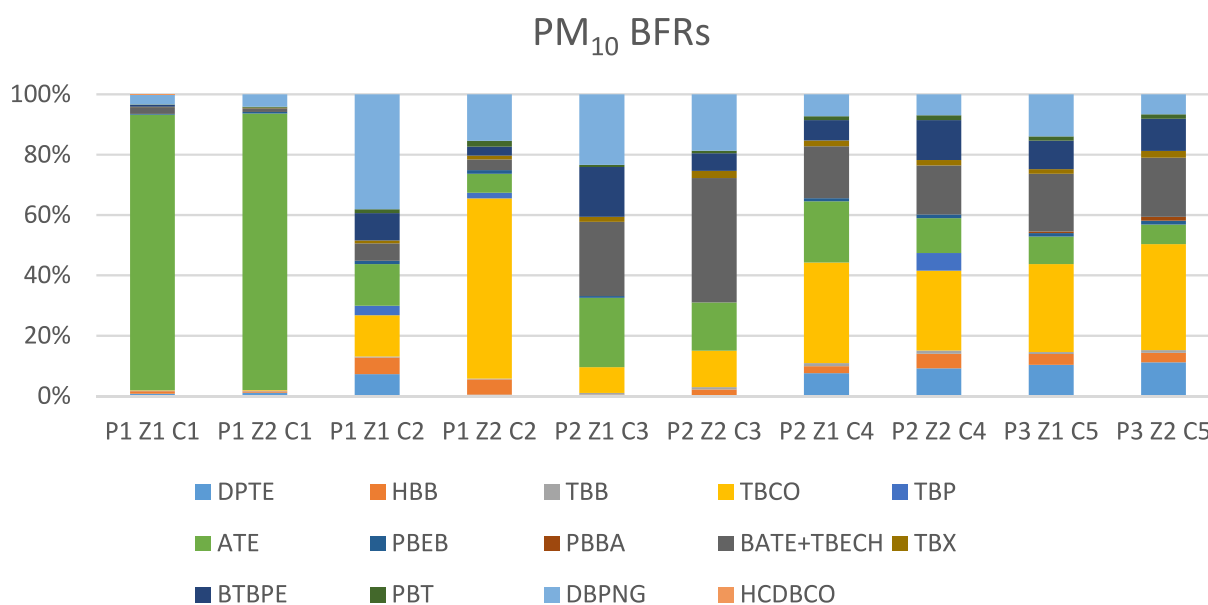
PM$_{10}$ BFRs

Fig. 7. Percentage of each compound to the total BFRs in PM$_{10}$ (compound names and corresponding abbreviations can be found in Supplementary Materials).

respectively prohibited by law [Law et al., 2014]. DBPNG (PM$_{10}$ concentration range 1.7–3.2 ng/m^3) is used as a flame retardant in unsaturated polyester resins, for molded products and rigid polyurethane foams. For TBCO, a toxicological concern exists but human biomonitoring data are not available. ATE is in the list of priority chemicals but a toxicity profile is not available; data on observations in humans exposed to DBNPG are not available. In ultrafine particles, TBCO and DBNPG concentrations are slightly above 1 ng/m^3, but ATE concentration reaches the non-negligible value of 21.3 ng/m^3.

The histogram in Fig. 8 shows the oxy-PAH percentage. Naphthalic anhydride (PM$_{10}$ concentration 2–48 ng/m^3), is the oxyPAH with a higher percentage distribution compared to all monitored oxy-PAHs. Along with being the oxidation product of the reactions of three-ring PAHs, 1,8-NapAnh, is an industrial chemical product for the large-scale production of plasticizers [Lorz et al., 2007].

The second more concentrated oxy-PAH is 9-fluorenone (concentration range in PM$_{10}$ 1–35 ng/m^3). Its presence may depend on the

incomplete combustion of the diesel engines of the trucks, which are stationed outside the plants, and of the forklifts, which transport waste inside the structure. Furthermore, its predominance is justified in its use in the production of polyradicals for resins and in its important function as a metallocene catalyst (as a binder). Metallocenes are of industrial interest in the context of catalysis for the production of polymers.

Finally, the third for concentration is 9,10-anthraquinone which is used for its semiconductor characteristics in manufactured articles.

Oxygenated PAHs are toxicologically relevant but neglected pollutants that have been shown to induce oxidative stress, endocrine system disruptions, and cytotoxic effects in mammalian cell systems. In addition, several oxyPAHs have been shown to elicit mutagenic [Lundstedt et al., 2007; Di Filippo et al., 2015].

Regarding oxy-PAHs found at higher concentrations in the sites under study, no significant toxicity is observed for naphthalic anhydride in the available studies. The overall toxicological risk from human exposure to anthraquinone is considered negligible, and no occupational
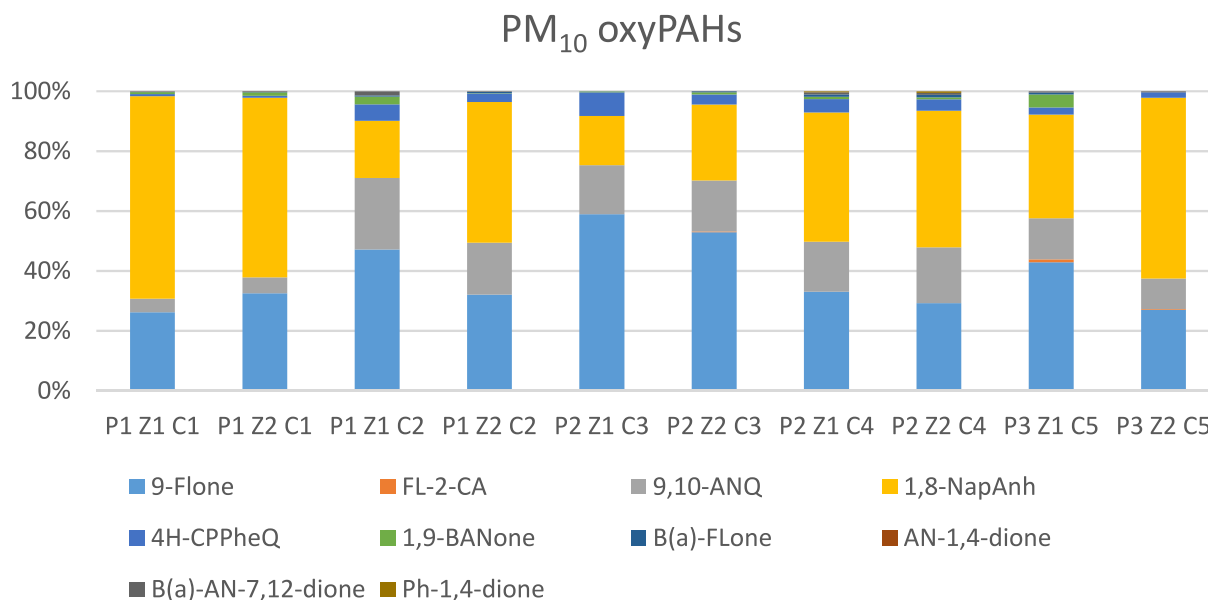
PM$_{10}$ oxyPAHs

Fig. 8. Percentage of each compound to the total oxyPAHs in PM$_{10}$ (compound names and corresponding abbreviations can be found in Supplementary Materials).
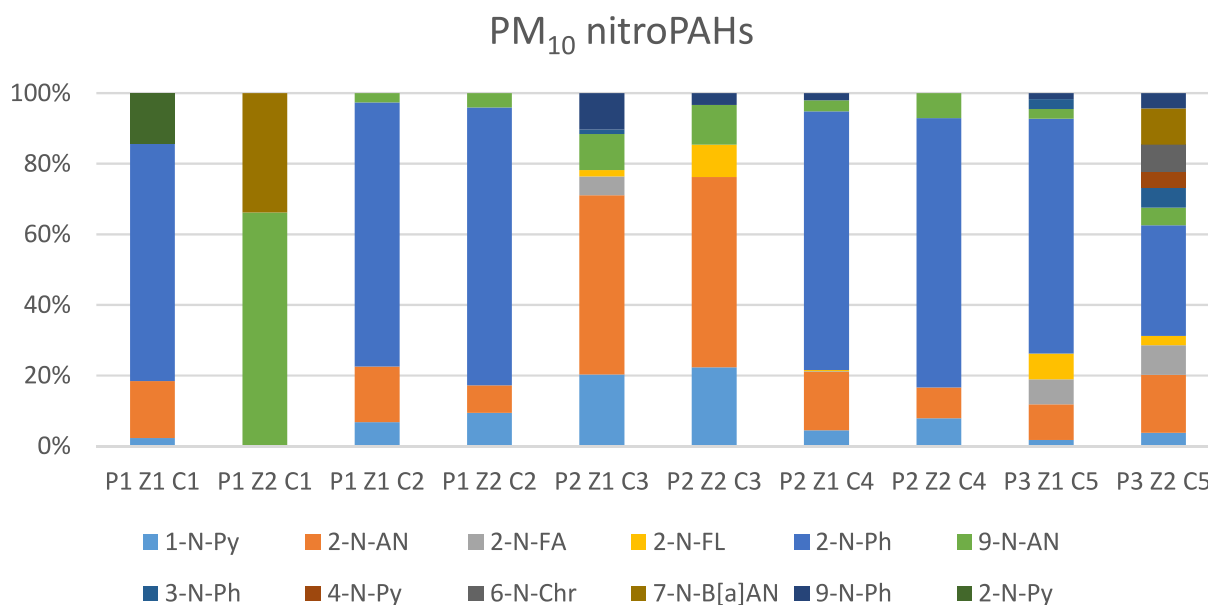
PM$_{10}$ nitroPAHs

Fig. 9. Percentage of each compound to the total nitroPAHs in PM$_{10}$ (compound names and corresponding abbreviations can be found in Supplementary Materials).

exposure limits have been derived by the American Conference of Governmental Industrial Hygienists. On the contrary, the toxicological properties of 9-fluorenone have not been fully investigated, but is considered hazardous by the 2012 OSHA Hazard Communication Standard, since animal studies have reported the development of tumors in case of chronic exposure. The higher concentration found in the ultrafine particles is 8.6 ng/m^3 in P3 Z1 C5.

The histogram in Fig. 9 shows the nitro-PAHs relative proportion. 2-nitrophenanthrene (2.3 ng/m^3) and 2-nitroanthracene (0.7 ng/m^3) maximum values are found in the PM$_{10}$ of P3_Z1 and P3_Z2, respectively. Depending on the site, 2-N-Ph and 2-N-AN are the most abundant nitro-IPAs and their origin essentially from diesel dust must be questioned given the low concentrations of 1-nitropyrene usually the predominant component of nitro-PAH in diesel emissions (10–100 times more abundant than the other nitro-PAHs). It has been shown that nitration on pyrene adsorbed on acid surfaces acting as catalysts occurs by nitrogen dioxide [Kameda, 2018]. It has been also shown the

nitration of phenanthrene and anthracene accelerated on acidic surfaces that can support nitration reactions where different nitrating species such as HNO$_2$ or HNO$_3$ may be involved [Heeb et al., 2008]. The prolonged exposure and the presence of compounds acting as catalysts, e.g., metal ions may support slower reactions. On the contrary, particle-associated 2-NPY only formed from gas-phase OH chemistry, doesn't occur in the present samples. Pyrene, fluoranthene and anthracene precursors are not carcinogenic, but nitroderivatives are classified as direct-acting mutagens, and for them there is no lower limit of exposure [Heeb et al., 2008]. Thus, even if nitroPAH concentrations are very low (PM$_{0.1}$-bound 2-N-AN and 2-N-Ph concentrations up to 0.14 and 1.47 ng/m^3, respectively), their contribution cannot be neglected.

Finally, the histogram in Fig. 10 shows the relative proportion of PFASs in all the areas. Of the 26 PFASs initially included in the monitoring, only the five PFASs shown in Fig. 10 are identified and the PFASs detected are different depending on the zone. High concentrations are found in P1_Z1_C2, P2_Z1_C3 and P2_Z1_C4 and always due to a single
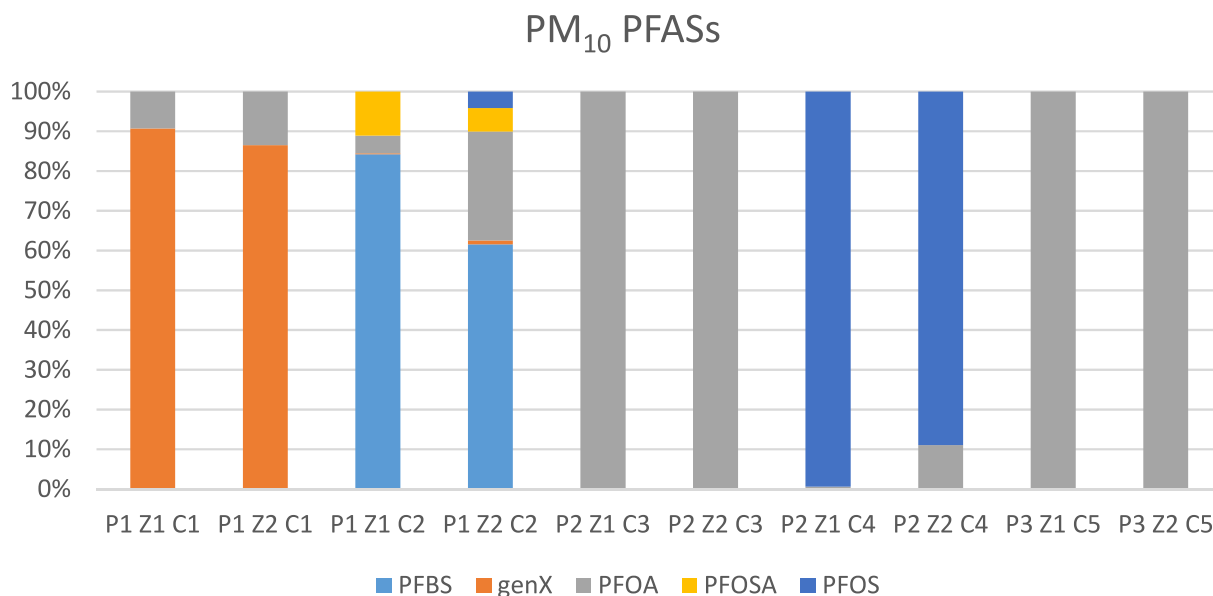
Fig. 10. Percentage of each compound to the total PFASs in PM$_{10}$ (compound names and corresponding abbreviations can be found in Supplementary Materials).

PFAS. As already stated, we found very high concentrations of PFBS in P1_Z1_C2 and P2_Z1_C3 (313 and 268 ng/m^3, respectively) and a high concentration of PFOS in PM$_{10}$ of P2_Z1_C4 (409 ng/m^3). Moreover, in PM$_{10}$ sampled in P1_Z1_C2 we also found PFOSA with a maximum of 41 ng/m^3; the genX with a maximum of 24 ng/m^3 is found in PM$_{10}$ of P1_Z1_C1. PFOA with a maximum of 23 ng/m^3 is found in PM$_{10}$ in P1_Z2_C2 (shredding of glass component) together with smaller amount

of PFBS and GenX. Smaller quantities are found in the second campaign (C4) of P2 and in P3. In P3, where tearing washing machines and crushing lamps, only PFOA is detected, at concentrations of 7 and 13 ng/m^3, respectively. PFOA in the range 2–23 ng/m^3 is of the same or 1 order of greatness higher than in airborne particles collected from kindergartens in Hong Kong [Li et al., 2021].

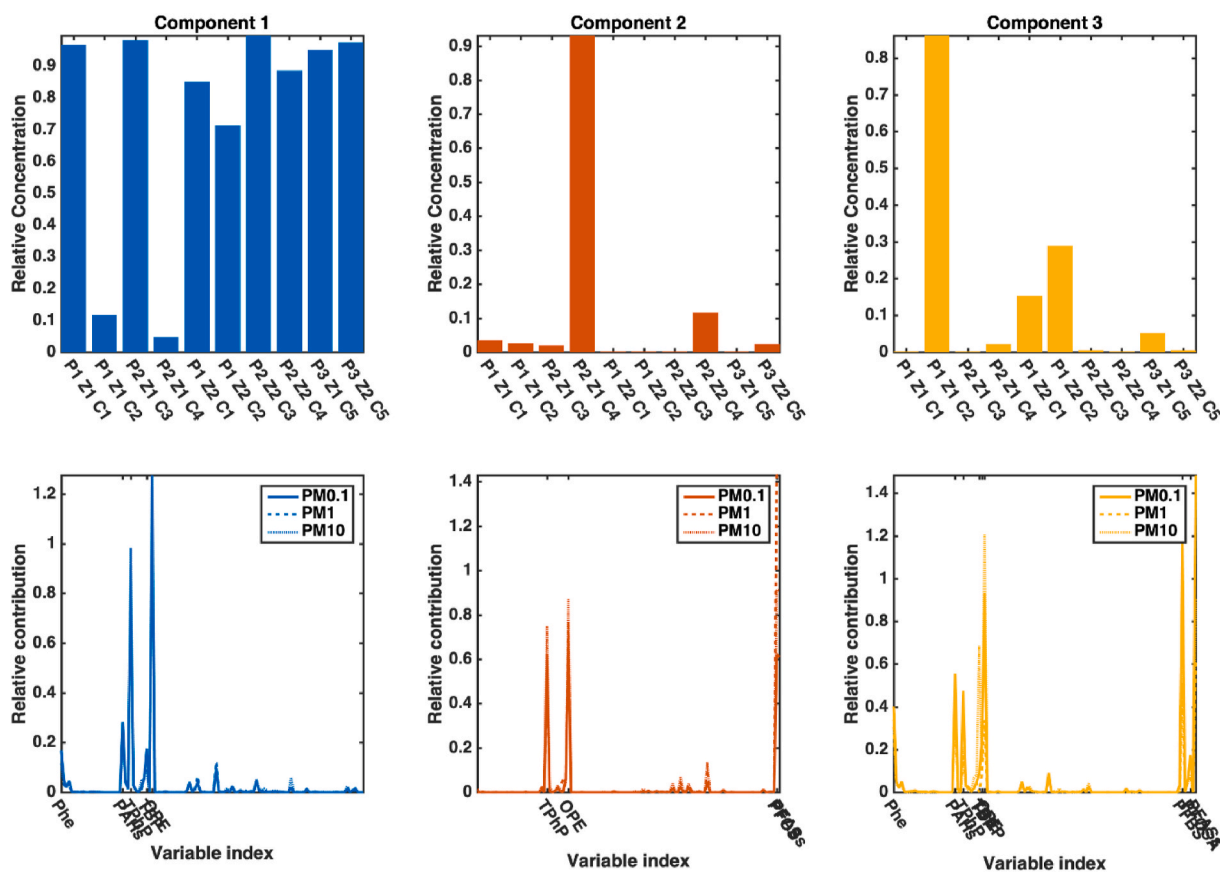Poly- and perfluorinated alkyl substances (PFAS) are used in

Fig. 11. Source apportionment by MCR analysis. Relative contribution (upper panels) and chemical profiles (lower panels) of the three components extracted by the MCR-ALS analysis.

electronic products due to their unique properties that improve product quality and performance [Tansel, 2022]. During handling and processing of PFAS-contaminated products (e.g. flat panel displays, liquid crystal displays, sensors, wire and cables, Printed Circuit Boards), PFAS exposure can occur by inhalation of particles released [Tansel, 2022 and references therein]. These results, therefore, have led us to the hypothesis that PFAS presence in PM is due to emissions from differently contaminated products. PFASs show non-negligible concentrations even in the ultrafine fraction of particles: PFBS, genX, PFOA, PFOSA and PFOS higher concentrations found in $PM_{0.1}$ are 128.4, 9.6, 7.8, 17.9, 64.8, and 151.5 ng/m^3, respectively. PFAS are in the REACH (Registration, Evaluation, Authorisation and Restriction of Chemicals) list of substances of very high concern (SVHC), based on their persistence, mobility and toxicity. Among PFASs identified as of equivalent concern to carcinogens, mutagens and reprotoxicants and persistent, bioaccumulative and toxic/very persistent and very bioaccumulative chemicals, there are the five PFASs found in the ultrafine fraction.

3.4. Statistical analysis results

Fig. 11 depicts the results of MCR analysis on the collected experimental data. Inspection of the Figure allows unraveling which individual compound and classes of compounds mainly contribute to the organic content in each site and in each campaign and in the different fractions of PM in each sampling location.

In all sites, except in P1_Z1_C2 and P2_Z1_C4, about 90% of the contribution to the content of organic compounds is characterized by PAHs with Phe and by OPEs with TPhP and TBP (first component, blue bars and lines). Furthermore, in P2_Z1_C4, PFASs with the PFOS also make a decisive contribution (second component, orange bars and lines). Lastly, in P1_Z1_C1, a further contribution is given by PFBS and PFOSA among PFASs, and TCEP among OPEs (third component, yellow bars and lines). $PM_{0.1}$, $PM_{0.1-1}$ and PM_{1-10} do not show significant differences.

4. Conclusions

Mechanical grinding and shredding operations in WEEE treatment plants cause the spread of airborne particles of different size. These particles contain toxic compounds, coming from electric circuits, electronic components, lamps, household appliances, and polymers as common material used for electric and electronic equipment housings. We investigated three different WEEE treatment facilities, where ultrafine, fine and coarse PM was collected and analyzed for organic compounds. Flame retardants and products from incomplete combustion were extracted and analyzed in GC/MS or HPLC/MS-MS. Coarse PM mass concentrations were always higher than the finer particles. $PM_{0.1}$ concentrations ranged between 12 and 64 $\mu g/m^3$; $PM_{0.1-1}$ concentrations, ranged from 46 to 125 $\mu g/m^3$, and PM_{1-10} concentration range was 70–544 $\mu g/m^3$. The concentrations of toxins absorbed on particles were of the order of tens or hundreds of ng/m^3. On average, 27% of the organic compounds found were distributed in the ultrafine fraction of PM (concentration range 96–342 ng/m^3).

The presence of toxic compounds in the ultrafine fraction of PM certainly raises questions about exposure even if the doses are low, due to the presence of many compounds and the possible long exposure times, as well as the possibility to be delivered to target organs The presence of ultrafine particles is not sufficiently studied for its contribution of toxicity. Specific cohort studies both for the presence of ultrafine particles in indoor atmosphere and for the workers of WEEE plants must certainly be encouraged.

Author contributions statements

Role of Authors: All the authors have contributed to the conception and design of the work, to the acquisition, analysis, and interpretation of data. All the authors have given the final approval of the version to be published, after agreement on all aspects of the work.

Declaration of competing interest

All the authors declare no actual or potential conflicts of interest regarding the submitted manuscript.

Data availability

Data will be made available on request.

Appendix A. Supplementary data

Supplementary data to this article can be found online at https://doi.org/10.1016/j.chemosphere.2023.139443.

References

Alassali, A., Calmano, W., Gidarakos, E., Kuchta, K., 2020. The degree and source of plastic reclyclates contamination with polycyclic aromatic hydrocarbons. RSC Adv. 10, 44989–44996. https://doi.org/10.1039/D0RA08554E.

Arp, H.P.H., Morin, N.A., Andersson, P.L., Hale, S.E., Wania, F., Breivik, K., Breedveld, G.D., 2020. The presence, emission and partitioning behavior of polychlorinated biphenyls in waste, leachate and aerosols from Norwegian waste-handling facilities. Sci. Total Environ. 715, 136824 https://doi.org/10.1016/j.scitotenv.2020.136824.

Balasch, A., López, M., Reche, C., Viana, M., Moreno, T., Eljarrat, E., 2022. Exposure of e-waste dismantlers from a formal recycling facility in Spain to inhalable organophosphate and halogenated flame retardants. Chemosphere 294, 133775. https://doi.org/10.1016/j.chemosphere.2022.133775.

Buiarelli, F., Di Filippo, P., Massimi, L., Pomata, D., Riccardi, C., Simonetti, G., Sonego, E., 2019. Ultrafine, fine and coarse airborne particle mass concentration in workplaces. Atmos. Pollut. Res. 10 (5), 1685–1690. https://doi.org/10.1016/j.apr.2019.06.009.

Buiarelli, F., Di Filippo, P., Pomata, D., Riccardi, C., Bartocci, M., 2017. A liquid chromatography tandem mass spectrometry method for simultaneous analysis of 46 atmospheric particulate-phase persistent organic pollutants and comparison with gas chromatography/mass spectrometry. Int. J. Environ. Anal. Chem. 97 (9), 797–818. https://doi.org/10.1080/03067319.2017.1369535.

Cabada, J.C., Rees, S., Takahama, S., Khlystov, A., Pandis, S.N., Davidson, C.I., Robinson, A.L., 2004. Mass size distributions and size resolved chemical composition of fine particulate matter at the Pittsburgh supersite. Atmos. Environ. 38 (20), 3127–3141. https://doi.org/10.1016/j.atmosenv.2004.03.004.

Candelmo, A.C., Deshpande, A., Dockum, B., et al., 2010. The effect of contaminated prey on feeding, activity, and growth of young-of-the-year bluefish, pomatomus saltatrix, in the laboratory. Estuar. Coast 33, 1025–1038. https://doi.org/10.1007/s12237-010-9292-3.

Cattley, RC, Kromhou, H, Sun, M, Tokar, EJ, Abdallah, MA, Bauer, AK, Broadwater, KR, Campo, L, Corsini, E, Houck, KA, Ichihara, G, Matsumoto, M, Morais, S, Mráz, J, Nomiyama, T, Ryan, K, Shen, H, Toyoda, T, Vähäkangas, K, Yakubovskaya, MG, Yu, IJ, DeBono, NL, de Conti, A, Ghissassi, FE, Madia, F, Mattock, H, Pasqual, E, Suonio, E, Wedekind, R, Benbrahim-Tallaa, L, Schubauer-Berigan, MK, 2023. Carcinogenicity of anthracene, 2-bromopropane, butyl methacrylate, and dimethyl hydrogen phosphite. The Lancet Oncology 24 (5), 431–432. https://doi.org/10.1016/S1470-2045(23)00141-9.

Chaine, C., Hursthouse, A.S., McLean, B., McLellan, I., McMahon, B., McNulty, J., Miller, J., Viza, E., 2022. Recycling plastics from WEEE: a review of the environmental and human health challenges associated with brominated flame retardants. Int. J. Environ. Res. Publ. Health 19, 766. https://doi.org/10.3390/ijerph19020766.

Chen, R., Shi, X., Bai, Ru, Rang, W., Huo, L., Zhao, L., Long, D., Pui, D.Y.H., Chen, C., 2015. Airborne nanoparticle pollution in a wire electrical discharge machining workshop and potential health risks. Aerosol Air Qual. Res. 15 (1), 284–294. https://doi.org/10.4209/aaqr.2014.09.0219.

Di Filippo, P., Pomata, D., Riccardi, C., Buiarelli, F., Gallo, V., 2015. Oxygenated polycyclic aromatic hydrocarbons in size-segregated urban aerosol. J. Aerosol Sci. 87, 126–134. https://doi.org/10.1016/j.jaerosci.2015.05.008.

De Juan, A., Jaumot, J., Tauler, R., 2014. Multivariate Curve Resolution (MCR). Solving the mixture analysis problem. Anal. Methods 6, 4964. https://pubs.rsc.org/en/content/articlelanding/2014/AY/C4AY00571F.

Di Filippo, P., Riccardi, C., Pomata, D., Buiarelli, F., 2010. Concentrations of PAHs, and nitro- and methyl- derivatives associated with a size-segregated urban aerosol. Atmos. Environ. 44 (23), 2742–2749. https://doi.org/10.1016/j.atmosenv.2010.04.035.

Esplugas, R., Rovira, J., Mari, M., Fernández-Arribas, J., Eljarrat, E., Domingo, J.L., Schuhmacher, M., 2022. Emerging and legacy flame retardants in indoor air and dust samples of Tarragona Province (Catalonia, Spain). Sci. Total Environ. 806, 150494 https://doi.org/10.1016/j.scitotenv.2021.150494.

Fjäder, P., Turunen, T., Rinne, P., Häkkinen, E., Kauppi, S., Sormunen, T., Andersson, M., 2022a. Reports of the Finnish Environment Institute 33 (Finnish Environment Institute; Centre for Sustainable Consumption and Production; Subject Editor: Ari Nissinen; syke.fi/publications | helda.helsinki.fi/syke).

Gugamsetty, B., Wei, H., Liu, C.N., Awasthi, A., Hsu, S.C., Tsai, C.J., Roam, G.D., Wu, Y. C., Chen, C.F., 2012. Source characterization and apportionment of PM_{10}, $PM_{2.5}$ and $PM_{0.1}$ by using positive matrix factorization. Aerosol Air Qual. Res. 12, 476–491. https://doi.org/10.4209/aaqr.2012.04.0084.

Heeb, N.V., Schmid, P., Kohler, M., Gujer, E., Zennegg, M., Wenger, D., Wichser, A., Ulrich, A., Gfeller, U., Honegger, P., Zeyer, K., Emmenegger, L., Petermann, J.-L., Czerwinski, J., Mosimann, T., Kasper, M., Mayer, A., 2008. Secondary effects of catalytic diesel particulate filters: conversion of PAHs versus formation of nitro-PAHs. Environ. Sci. Technol. 42, 3773–3779. https://doi.org/10.1021/es7026949.

Jiang, X., Xu, F., Qiu, X., Shi, X., Pardo, M., Shang, Y., Wang, J., Rudich, Y., Zhu, T., 2019. Hydrophobic organic components of ambient fine particulate matter (PM2.5) associated with inflammatory cellular response. Environ. Sci. Technol. 53 (17), 10479–10486. https://doi.org/10.1021/acs.est.9b02902.

Kameda, T., 2018. Atmospheric reactions of PAH derivatives: formation and degradation polycyclic aromatic hydrocarbons 75–91. In: Hayakawa, K. (Ed.), Polycyclic Aromatic Hydrocarbons. Springer, Singapore. https://doi.org/10.1007/978-981-10-6775-4_7.

Kim, Y.H., Wyrzykowska-Ceradini, B., Touati, A., Krantz, Q.T., Dye, J.A., Linak, W.P., Gullett, B., Gilmour, M.I., 2015. Characterization of size-fractionated airborne particles inside an electronic waste recycling facility and acute toxicity testing in mice. Environ. Sci. Technol. 49, 11543–11550. https://doi.org/10.1021/acs.est.5b03263.

Kwon, H.S., Ryu, M.H., Carlsten, C., 2020. Ultrafine particles: unique physicochemical properties relevant to health and disease. Exp. Mol. Med. 52, 318–328. https://doi.org/10.1038/s12276-020-0405-1.

Lassen, P., Hoffmann, L., Thomsen, M., 2012. PAHs in Toys and Childcare Products. National Environmental Research Institute Aarhus University. Roskilde Survey. Survey of Chemical Substances in Consumer. Danish Environmental Protection Agency. Products No. 114 2011. https://www2.mst.dk/udgiv/publications/2012/01/978-87-92779-49-6.pdf.

Law, R.J., Covaci, A., Harrad, S., Herzke, D., Abdallah, M.A.E., Fernie, K., Takigami, H., 2014. Levels and trends of PBDEs and HBCDs in the global environment: status at the end of 2012. Environ. Int. 65, 147–158. https://doi.org/10.1016/j.envint.2014.01.006.

Li, N., Ying, G.-G., Hong, H., Deng, W.-J., 2021. Perfluoroalkyl substances in the urine and hair of preschool children, airborne particles in kindergartens, and drinking water in Hong Kong. Environ. Pollut. 270, 116219 https://doi.org/10.1016/j.envpol.2020.116219.

Li, S.-Q., Ni, H.-G., Zeng, 2017. PAHs in polystyrene food contact materials: an unintended consequence. Sci. Total Environ. 609, 1126–1131. https://doi.org/10.1016/j.scitotenv.2017.07.262.

Lindstrom, A.B., Strynar, M.J., Libelo, E.L., 2011. Polyfluorinated compounds: past, present, and future. Environ. Sci. Technol. 45 (19), 7954–7961. https://doi.org/10.1021/es2011622.

López, M., Reche, C., Pérez-Albaladejo, E., Porte, C., Balasch, A., Monfort, E., Eljarrat, E., Viana, M., 2022. E-waste dismantling as a source of personal exposure and environmental release of fine and ultrafine particles. Sci. Total Environ. 833, 154871 https://doi.org/10.1016/j.scitotenv.2022.154871.

Lorz, P.M., Towae, F.K., Enke, W., Jäckh, R., Bhargava, N., Hillesheim, W., 2007. Phthalic Acid and Derivatives Ullmann's Encyclopedia of Industrial Chemistry. Wiley-VCH, Weinheim. https://doi.org/10.1002/14356007.a20_181.pub2.

Lundstedt, S., White, P.A., Lemieux, C.L., Lynes, K.D., Lambert, I.B., Öberg, L., Haglund, P., Tysklind, M., 2007. Sources, fate, and toxic hazards of oxygenated polycyclic aromatic hydrocarbons (PAHs) at PAH contaminated sites. Ambio 36 (6), 475–485. https://doi.org/10.1579/0044-7447(2007)36[475:SFATHO]2.0.CO;2.

Montano, L., Pironti, C., Pinto, G., Ricciardi, M., Buono, A., Brogna, C., Venier, M., Piscopo, M., Amoresano, A., Motta, O., 2022. Polychlorinated biphenyls (PCBs) in the environment: occupational and exposure events, effects on human health and fertility. Toxics 10, 365. https://doi.org/10.3390/toxics10070365.

Morf, L.S., Tremp, J., Gloor, R., Huber, Y., Stengele, M., Zennegg, M., 2005. Brominated flame retardants in waste electrical and electronic equipment: substance flows in a recycling plant. Environ. Sci. Technol. 39 (22), 8691–8699. https://doi.org/10.1021/es051170k.

Morin, N.A.O., Andersson, P.L., Hale, S.E., Arp, H.P.H., 2017. The presence and partitioning behavior of flame retardants in waste, leachate, and air particles from Norwegian waste-handling facilities. J. Environ. Sci. 62, 115–132. https://doi.org/10.1016/j.jes.2017.09.005.

Nguyen, L.V., Diamond, M.L., Venier, M., Stubbings, W.A., Romanak, K., Bajard, L., Melymuk, L., Jantunen, L.M., 2019. Arrandal VH Exposure of Canadian electronic waste dismantlers to flame retardants. Environ. Int. 129, 95–104. https://doi.org/10.1016/j.envint.2019.04.056.

Pazzi, G., Buiarelli, F., Di Filippo, P., Pomata, D., Riccardi, C., Lucarelli, F., Giardi, F., Sonego, E., Galarini, R., Lorenzetti, S., Goracci, L., Simonetti, G., 2023. Metals and organic species associated with fine and coarse aerosol particles in an electronic waste recycling plant. Air Quality, Atmosphere & Health 1–16. https://doi.org/10.1007/s11869-023-01313-4.

Papaoikonomou, K., Emmanouil, C., Vasilatou, V., Diapouli, E., Grigoratos, T., Zafirakou, A., Kungolos, A., 2018. PM_{10} and elemental concentrations in a dismantling plant for waste of electrical and electronic equipment in Greece. Aerosol Air Qual. Res. 18, 1457–1469. https://doi.org/10.4209/aaqr.2017.12.0557.

Pomata, D., Di Filippo, P., Riccardi, C., Castellani, F., Simonetti, G., Sonego, E., Buiarelli, F., 2021. Toxic organic contaminants in airborne particles: levels, potential sources and risk assessment. Int. J. Environ. Res. Publ. Health 18 (8), 4352. https://doi.org/10.3390/ijerph18084352.

Pomata, D., Di Filippo, P., Riccardi, C., Rossi, V., Simonetti, G., Sonego, E., Buiarelli, F., 2020. Method optimisation for the simultaneous determination of legacy and emerging halogenated flame retardants in particulate matter collected in an electronic waste recycling facility. Int. J. Environ. Anal. Chem. 100 (13), 1479–1496. https://doi.org/10.1080/03067319.2019.1655007.

Rahman, F., Langford, K.H., Scrimshaw, M.D., Lester, J.N., 2001. Review. Polybrominated diphenyl ether (PBDE) flame retardants. Sci. Total Environ. 275, 1–17. https://doi.org/10.1016/s0048-9697(01)00852-x.

Roth, T., Bertran, R.U., Pöhlein, M., Wolf, M., van Eldik, R., 2012. Gas chromatographic determination of phosphate-based flame retardants in styrene-based polymers from waste electrical and electronic equipment. J. Chromatogr. A 1262, 188–195. https://doi.org/10.1016/j.chroma.2012.08.070.

Safe, S.H., 1997. Is there an association between exposure to environmental estrogens and breast cancer? Environ. Health Perspect. 105, 675–678. https://doi.org/10.2307/3433388.

Sardar, S.B., Fine, P.M., Mayo, P.R., Sioutas, C., 2005. Size-fractionated measurements of ambient ultrafine particle chemical composition in los angeles using the NanoMOUDI. Environ. Sci. Technol. 39 (4), 932–944. https://doi.org/10.1021/es049478j.

Sharkey, M., Harrad, S., Abdallah, A.-E.M., Drage, D.S., Berresheim, H., 2020. Phasing-out of legacy brominated flame retardants: the UNEP Stockholm Convention and other legislative action worldwide. Environ. Int. 144, 106041 https://doi.org/10.1016/j.envint.2020.106041.

Schober, W., Pusch, G., Oeder, S., Reindl, H., Behrendt, H., Buters, J.T.M., 2010. Metabolic activation of phenanthrene by human and mouse cytochromes P450 and pharmacokinetics in CYP1A2 knockout mice. Chem. Biol. Interact. 183 (1), 57–66. https://doi.org/10.1016/j.cbi.2009.09.008.

Schraufnagel, D.E., 2020. The health effects of ultrafine particles. Exp. Mol. Med. 52, 311–317. https://doi.org/10.1038/s12276-020-0403-3.

Shi, J., Xiang, L., Luan, H., Wei, Y., Ren, H., Chen, P., 2019. The health concern of polychlorinated biphenyls (PCBs) in a notorious e-waste recycling site. Ecotoxicol. Environ. Saf. 186, 109817 https://doi.org/10.1016/j.ecoenv.2019.109817.

Sima, M.W., Jaffé, P.R., 2021. A critical review of modeling Poly- and Perfluoroalkyl Substances (PFAS) in the soil-water environment. Sci. Total Environ. 757, 143793 https://doi.org/10.1016/j.scitotenv.2020.143793.

Simonetti, G., Di Filippo, P., Riccardi, C., Pomata, D., Sonego, E., Buiarelli, F., 2020. Occurrence of halogenated pollutants in domestic and occupational indoor dust. Int. J. Environ. Res. Publ. Health 17 (11), 3813. https://doi.org/10.3390/ijerph17113813.

Smichowski, P., Gómez, D.R., 2023. An overview of natural and anthropogenic sources of ultrafine airborne particles: analytical determination to assess the multielemental profiles. Appl. Spectrosc. Rev. 1–27 https://doi.org/10.1080/05704928.2023.2166522.

Sonego, E., Simonetti, G., Di Filippo, P., Riccardi, C., Buiarelli, F., Fresta, A., Olivastri, M., Pomata, D., 2022. Characterization of organophosphate esters (OPEs) and polyfluoralkyl substances (PFASs) in settled dust in specific workplaces. Environ. Sci. Pollut. Control Ser. 29, 52302–52316. https://doi.org/10.1007/s11356-022-19486-3.

Suresh, S.S., Bonda, S., Mohanty, S., Nayak, S.K., 2018. A review on computer waste with its special insight to toxic elements, segregation and recycling techniques. Process Saf. Environ. Protect. 116, 477–493. https://doi.org/10.1016/j.psep.2018.03.003.

Stubbings, W.A., Abdallah, M.A.-E., Misiuta, K., Onwuamaegbu, U., Holland, J., Smith, L., Parkinson, C., McKinlay, R., Harrad, S., 2021. Assessment of Brominated Flame Retardants in a Small Mixed Waste Electronic and Electrical Equipment (WEEE) Plastic Recycling Stream in the UK, vol. 780. Science of The Total Environment. https://doi.org/10.1016/j.scitotenv.2021.146543.

Stubbings, W.A., Nguyen, L.V., Romanak, K., Jantunen, L., Melymuk, L., Arrandale, V., Diamond, M.L., Venier, M., 2019. Flame retardants and plasticizers in a Canadian waste electrical and electronic equipment (WEEE) dismantling facility. Sci. Total Environ. 675, 594–603. https://doi.org/10.1016/j.scitotenv.2019.04.265.

Strobl, L., Diefenhardt, T., Schlummer, M., Leege, T., Wagner, S., 2021. Recycling potential for non-valorized plastic fractions from electrical and electronic waste. Recycling 6, 33. https://doi.org/10.3390/recycling6020033.

Tansel, B., 2022. PFAS use in electronic products and exposure risks during handling and processing of e-waste: a review. J. Environ. Manag. 316, 115291 https://doi.org/10.1016/j.jenvman.2022.115291.

Tsydenova, O., Bengtsson, M., 2011. Chemical hazards associated with treatment of waste electrical and electronic equipment. Waste Manag. 31 (1), 45–58. https://doi.org/10.1016/j.wasman.2010.08.014.

Vazquez-Pufleau, M., 2022. Venturi pump-critical orifice as an online and robust nanoparticle dilution probe for in situ powder stream characterization. Powder Technol. 412, 117974 https://doi.org/10.1016/j.powtec.2022.117974.

Viitanen, A.-K., Uuksulainen, S., Koivisto, A.J., Hämeri, K., Kauppinen, T., 2017. Workplace measurements of ultrafine particles—a literature review. Annals of Work Exposures and Health 61 (7). https://doi.org/10.1093/annweh/wxx049.

Weschler, C.J., 2011. Commemorating 20 years of indoor air chemistry in indoor environments: 20 years of research. Indoor Air 21, 205–218. https://doi.org/10.1111/j.1600-0668.2011.00713.x205.

Yang H, Shi Z, Wang X-X, Cheng R, Lu M, Zhu J, Deng W, Zeng Y, Zhao L-Y, Zhang S-Y. Phenanthrene, but not its isomer anthracene, effectively activates both human and mouse nuclear receptor constitutive androstane receptor (CAR) and induces hepatotoxicity in mice. Toxicol. Appl. Pharmacol.. 2019 378, 114618, https://doi.org/10.1016/j.taap.2019.114618.

Young, L.H., Lin, Y.H., Lin, T.H., Tsai, P.J., Wang, Y.F., Hung, S.M., Tsai, C.J., Chen, C.W., 2013. Field application of a newly developed personal nanoparticle sampler to selected metalworking operations. Aerosol Air Qual. Res. 13 (3), 849–861. https://doi.org/10.4209/aaqr.2012.10.0270.